INMM & ESARDA Joint Annual Meeting 2021 Paper
Facility Operations, Nuclear Archiving & Forensics

# COMPARING FEMTOSECOND LIBS UV-VIS SPECTRUM OF TRACE ELEMENTS IN SYNTHETIC NUCLEAR MELT GLASS AND TRINITITE FOR NUCLEAR FORENSICS

**J. Daniel Hartman**[1,2,3], Benjamin S. Jordan[1,2], Dean Forrest[1,2], Elijah J. Rosenburg[1,2], Howard L. Hall[1,2,3]

[1]Department of Nuclear Engineering, University of Tennessee, Knoxville, TN, USA, [2]Institute for Nuclear Security, University of Tennessee, Knoxville, TN, USA, [3]The Bredesen Center for Interdisciplinary Research and Graduate Education, Knoxville, TN, USA

## ABSTRACT

On July 16, 1945, the very first atomic (nuclear) bomb was detonated at the Trinity Test Site in Alamogordo, New Mexico. The sandy ground that surrounded the atomic bomb test site was heated to a temperature hotter than the sun and transformed into a geologic medium known as Trinitite (nuclear melt glass). Over 75 years and eight additional nuclear weapon possessing states later, the need to accurately ascertain the origins of nuclear weapons material in a timely manner (nuclear forensics) has never been more important. A surge in nuclear forensics research requiring trinitite over the past couple of decades led to a search for an accurate surrogate material. Recent work at the University of Tennessee Knoxville has resulted in the successful synthetization of nuclear melt glass, whose elemental composition closely resembles that of authentic Trinitite. This paper will introduce a novel comparison of the Ultraviolet-Visible spectrum (300-500 nm) of the Laser Induced Breakdown Spectroscopy (LIBS) of trace elements in synthetic (radioactive and non-radioactive) nuclear melt glass and authentic trinitite with a Femtosecond (Fs) laser. Accounting for the exception of the purposeful absence of uranium in the non-radioactive melt glass, unique characteristic peaks for all ten elements which make up trinitite were found in each of the three various sample types and subsequently cross referenced through use of the U.S. National Institute of Standards and Technology (NIST) LIBS database and past published Fs-LIBS literature. For this stage of the research our goal was to evaluate the ability of Fs-LIBS to identify the presence of elements in the trinitite and synthetic melt-glass that are only trace constituents of the overall composition on the material. This research paper will compare the spectral responses of trinitite and synthetic melt glass and will foreshadow the challenges of developing Fs-LIBS to the point of being able to attribute the weapon to a source based on the Fs-LIBS analysis of the trinitite. Additionally, we will report on laboratory testing techniques that were developed to provide spectra with improved signal-to-noise-ratios and the additional work needed to fully explain the plasma physics that have driven this result.

## INTRODUCTION

A 21-kiloton man-made atomic blast (codenamed Trinity) erupted into the Alamogordo, New Mexico sky early into the morning of July 16, 1945 to officially usher in the atomic age. This was the culminating efforts of over 3 years of extraordinary covert scientific research and development of the Manhattan Project during World War II in the United States. The intense heat of the atomic explosion melted the earth around ground zero of the Trinity test site which resulted in the creation and formation of nuclear melt glass or Trinitite. While various analytical methods were used soon thereafter and continued into the coming decades following the Trinity test to accurately determine and attribute specific radioisotopes and fission products from the atomic explosion, the application of nuclear forensics did not really explode into the scientific community until the 1990's shortly after the end of the Cold War which introduced the terrifying new global threat of nuclear terrorism.

[1] Corresponding Author E-mail address: jhartma7@vols.utk.edu

While mass spectrometry remains the global standard for isotopic analysis in the nuclear forensic community, there are a variety of other complimentary analytical techniques including Laser Induced Breakdown Spectroscopy (LIBS). In 1983, Radziemski was the first individual to employ LIBS for applied nuclear research in detecting Be in air [1]. Many other research groups have since utilized LIBS to assay uranium and other nuclear material in a variety of forms including uranium ore [2-5], uranium oxide/fuel [6-9], fission products [10-12], and spent fuel [13-19]. Other isotopic analysis research of uranium has been conducted by Doucet et al. [20] and by Cremers et al. [21]. Both investigated the shape of the U II line at 424.437 nm and tried to resolve the shift at that wavelength of U235 and U238 [20,21].

In addition to the promising results by the portable and field-deployable LIBS device of Cremers et al. [21], Shattan et al. [22] was the first to use a hand-held LIBS system to multi-element map both the exterior and an interior cross-section of surrogate nuclear debris for nuclear forensic applications. LIBS was also utilized to analytically measure environmental swipes taken by IAEA inspectors in Chinni et al. [23].

The only previous LIBS of Trinitite or synthetic nuclear melt glass was found in the appendix of a LIBS textbook by Cremers et al. [24]. Little information besides a few parameters for the ns-LIBS of Trinitite experiment were included in that textbook appendix and no origins for that ns-LIBS research could be found anywhere in open literature. The parameters for the ns-LIBS of Trinitite experiment were a laser beam energy of 54 mJ per pulse, delay time of 1.0 μs, gate width of 1.1 ms, 100 averaged spectra, and the use of a 75mm focal length lens [24]. It is worth noting that the elements in the range of 235-800nm found by that work were Si, Mg, Al, Ca, Ti, Na, H, N, K, and O, but only Al, Ca, Ti, and Na are within our spectrometer range of 300-500nm [24]. The NIST LIBS database was then consulted to compare the ns-LIBS spectrum found in the Cremers et al. textbook to validate that such an elemental spectrum would be expected if a Trinitite sample were ablated with a ns-laser [24]. Each of the elements found in this ns-LIBS of Trinitite work were found to be accurately represented in the NIST LIBS database [24].

In pursuit of an improved LIBS device for nuclear forensics, femtosecond lasers (fs-lasers) offer the advantages of higher sensitivity, low continuum emission, improved detection precision, minimal sample destruction, and a lower ablation energy threshold [25]. Additionally, the full energy of the fs-laser pulse is completely deposited into the target since there is no interaction of the beam with the laser induced plasma [26]. This lack of Laser Plasma Interaction (LPI) with a fs-laser eliminates the loss of any interrogated material before the emitted light can be collected [26]. Demonstrations of improvements in the use of non-gated detectors for analysis and the Limit Of Detection (LOD) for primary and trace elements in the sample have already been proven by the utilization of fs-lasers [26]. Current disadvantages of fs-lasers include the necessity of a highly controlled operating environment in addition to being larger, more expensive, and more complex than a ns-laser [25].

## METHODS

The primary equipment that was used for this research at the University of Tennessee Knoxville (UTK) included a Ti:Sapphire (Solstice-ACE-Prime-Plus) laser, ultrafast mirrors and a periscope (Thorlabs), sample chamber (Kimball Physics and KJ Lesker), a 70mm plano convex lens used to focus the laser inside the sample chamber (Thorlabs), two additional plano convex lenses (100mm and 25mm) for the collection optics assembly (Thorlabs), a reflective collimator (Thorlabs), fiber optic cable (Horiba), a 1250M-Series II spectrometer (Horiba), and a gateable Intensified Charge-Coupled Device (ICCD) (Andor). Parameters for this setup are in Table 1. An Oscilloscope and photo diode detector were used to determine that it takes 83 nanoseconds for the laser to reach the sample chamber. This time delay value of 83 nanoseconds was utilized to accurately reflect gating delays and widths for each experiment. The equipment setup that was used for this research is illustrated in Figure 1.

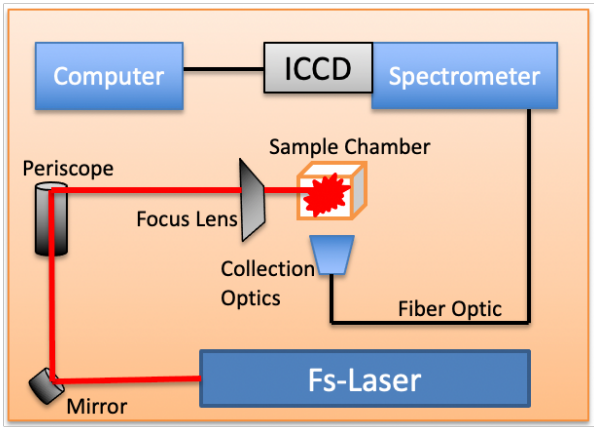


Figure 1 (above): Configuration of fs-laser lab setup.

| Table 1: Various Parameters (unless otherwise specified) of the primary equipment used for fs-LIBS experiments | |
|---|---|
| Laser Fundamental Wavelength | 800 nm |
| Laser Rep Rate | 1 kHz |
| Laser Pulse Width | 98 fs |
| Beam Diameter | 11 mm |
| Maximum laser beam pulse energy | 6 mJ |
| Focus lens (plano convex) | 75 mm |
| Spectrometer Focal length | 1.25 m |
| Spectrometer Slit Width | 20 µm |
| Spectrometer Grating | 3,600 grooves/mm |
| Spectrometer Resolution | 0.006 nm |
| Time for Laser to Reach Sample Chamber | 83 ns |
| Change in Sample Chamber Position via Stage Knob | 0.37mm/Half turn |

Fs-LIBS of Aluminum was chosen as a system benchmark to acquire distinguishable emission lines within the range of the spectrometer (300-500 nm). The Aluminum emission lines were expected to be very intense since the samples held within the epoxy discs were pure Aluminum alloys. These fs-LIBS of Aluminum experiments were then conducted to gain the necessary competence in fine-tuning various parameters for LIBS (gate delays, gate width, etc.) for future experiments with surrogate nuclear material and Trinitite. These various parameters were optimized to obtain the best experimental LIBS results [Maximize Signal to Noise Ratio (SNR) and minimize Relative Standard Deviation (RSD)].

After gaining sufficient confidence in fine-tuning the epoxy sample preparation techniques and the various LIBS parameters to maximize SNR and minimize RSD, attention was turned to conducting novel fs-LIBS of surrogate nuclear melt glass and authentic Trinitite. These optimizations were extremely important since the quantity and thickness of the non-radioactive nuclear melt glass samples were quite small. Surrogate non-radioactive nuclear melt glass samples had been synthesized at UTK by Molgaard et al. and were already set within epoxy samples so no further sample preparation was necessary [27]. The recipe for the Standard Trinitite Formation (STF) was developed by Molgaard et al. to replicate the average elemental composition of Trinitite from the Trinity Test in 1945 [27]. Table 2 illustrates the close resemblance of the two sample elemental compositions of non-radioactive analytes [27]. Table 2 and the NIST LIBS database were then examined to predict what peaks of interest should be investigated in the experiment. Table 3 contains each of the expected fs-LIBS emissions lines from each of the non-radioactive analytes in nuclear melt glass and Trinitite that should be interference free [28]. The radioactive STF samples also contain approximately 410 µg (micrograms) of natural uranium [27,29].

Table 2: Comparison of Non-Radioactive Elemental Composition of Trinitite vs. UTK Synthetic Nuclear Melt Glass [27]

| **Average Trinitite Data** | | **Standard Trinitite Formation (STF)** | |
|---|---|---|---|
| **Compound** | **Mass fraction** | **Compound** | **Mass fraction** |
| $SiO_2$ | 0.642 | $SiO_2$ | 0.642 |
| $Al_2O_3$ | 0.143 | $Al_2O_3$ | 0.143 |
| CaO | 0.0964 | CaO | 0.0964 |
| FeO | 0.0197 | FeO | 0.0197 |
| MgO | 0.0115 | MgO | 0.0115 |
| $Na_2O$ | 0.0125 | $Na_2O$ | 0.0125 |
| $K_2O$ | 0.0513 | $K_2O$ | 0.0612 |
| MnO | 0.000505 | MnO | 0.000505 |
| $TiO_2$ | 0.00427 | $TiO_2$ | 0.00427 |
| Total | 0.981 | Total | 0.991 |

Table 3: 16 Interference free analytical lines for analysis of trace elements in radioactive/non-radioactive nuclear melt glass and Trinitite [28]

| Peak (nm) | Analyte |
|---|---|
| 330.237 | Na I |
| 382.444 | Fe I |
| 382.935 | Mg I |
| 383.230 | Mg I |
| 383.829 | Mg I |
| 385.991 | Fe I |
| 390.552 | Si I |
| 394.741 | O I |
| 396.152 | Al I |
| 396.847 | Ca II |
| 403.075 | Mn I |
| 403.306 | Mn I |
| 403.448 | Mn I |
| 404.414 | K I |
| 422.672 | Ca I |
| 466.758 | Ti I |

Table 4: List of optimized gating parameters found from fs-LIBS experiments of synthetic nuclear melt glass (non-radioactive and radioactive) and Trinitite

| Analyte | $t_d$ (ns) | $t_g$ (ns) |
|---|---|---|
| Na I | 150 | 200 |
| Fe I | 100 | 200 |
| Mg I | 200 | 200 |
| Si I | 250 | 200 |
| Al I | 400 | 200 |
| O I | 275 | 200 |
| Ca I | 180 | 200 |
| Ca II | 400 | 200 |
| Mn I | 100 | 200 |
| K I | 180 | 200 |
| Ti I | 100 | 200 |

Sample preparation, transportation, and decontamination procedures for the synthetic nuclear melt glass (both non-radioactive and radioactive) and authentic Trinitite can be found in Appendix D [30]. Due to laser system limitations, it was not possible to leave the laser shutter open and subsequently fire a set amount of laser pulses to interrogate a sample as had been described in countless past LIBS literature. The procedure was to instead open and close the laser shutter rapidly (~ 1 sec) with one hand while simultaneously using the Andor software to acquire gated LIBS spectra with the use of the other hand. This LIBS acquisition technique was practiced, developed, and optimized from the very first experiments so that this experimental limitation would be minimized when collecting fs-LIBS data from the nuclear melt glass and Trinitite samples. The optimized gating parameters listed in Table 4 for each of the ten primary trace elements found in the surrogate nuclear melt glass and Trinitite samples were obtained by consulting past literature in addition to trial and error as many of the elements investigated in these experiments had little to no past published literature with fs-lasers in the range of interest for our spectrometer. An unablated radioactive melt glass sample is shown in figure 2 and figures 3-5 illustrate fs-LIBS of surrogate nuclear melt glass and Trinitite samples.

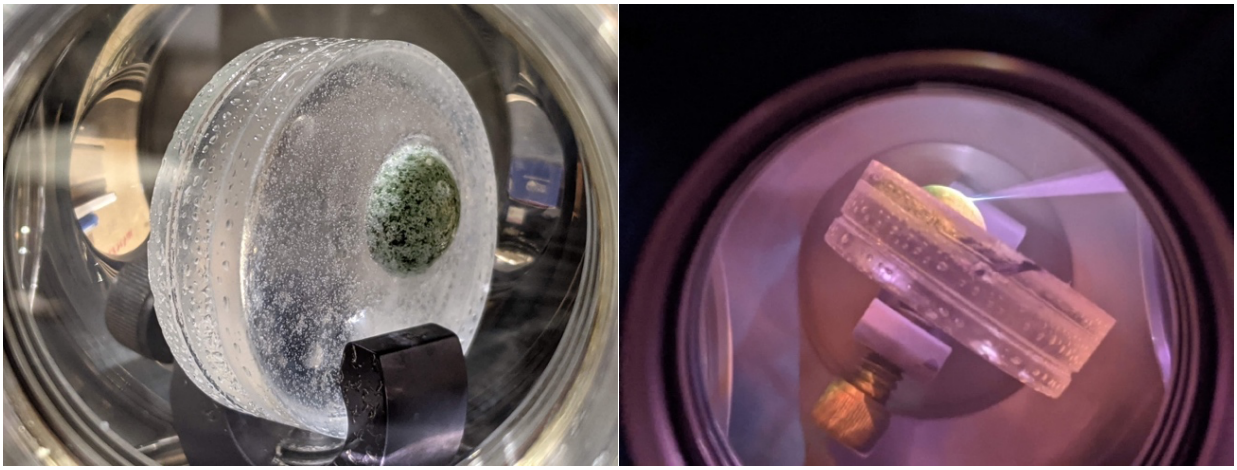

Figures 2 & 3: Radioactive melt glass, unablated (left) & during fs-LIBS (right).

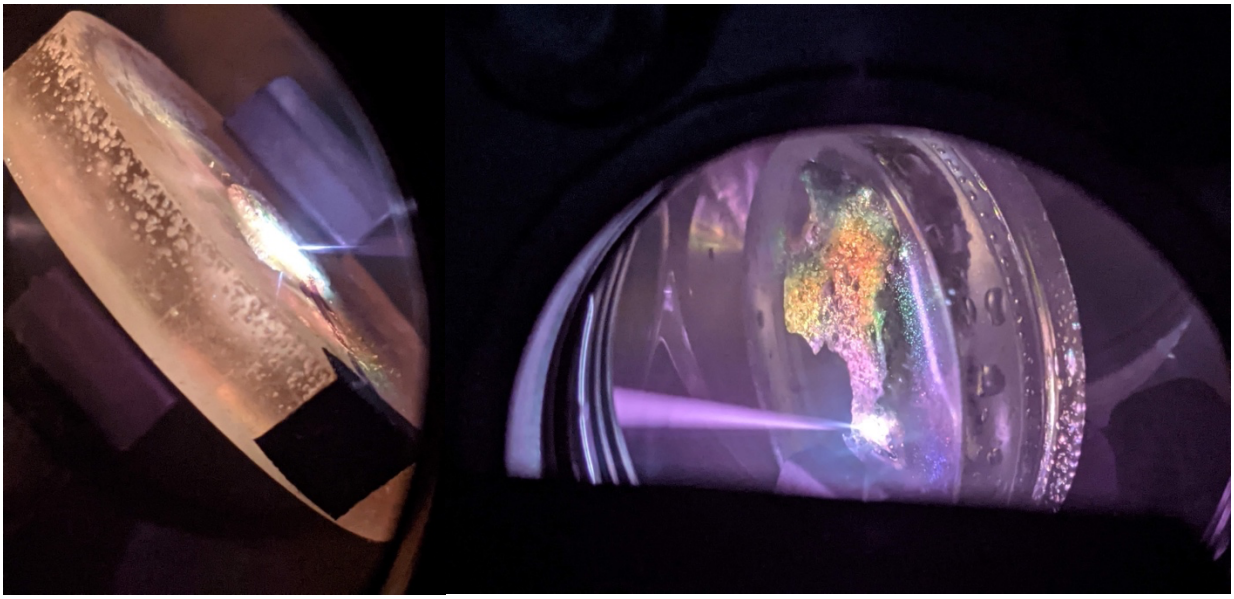

Figures 4 & 5: Fs-LIBS of non-radioactive melt glass (left) & Trinitite (right).

## RESULTS

With the raw spectral data in terms of pixels, with pixels being specific to the equipment, the conversion to a more general abscissa was required. To avoid generating a pixel-wavelength calibration curve for the spectrometer's entire range, from 300 to 500 nm, the LabSpec 6 spectroscopy suite was used to generate an abscissa, in terms of wavelength, that preserves the ICCD camera's resolution over the spectral range. Then, using a wavelength-wavelength calibration curve generated from Mercury lines, the wavelength of the range reported by the spectrometer was corrected.

Using this corrected abscissa, the conversion process for each pixel spectra used one of two methods, depending on the number of peaks present in the pixel-based spectra. For spectra with one known peak, the position of the peak's maximum height was lined up with an index in the spectrometer's reported abscissa. From there, the remaining noise in the pixel data was lined up with the spectrometer's reported abscissa. For spectra with more than a single peak, a calibration curve was generated for the specific pixel-based spectra to be converted. Once the calibration curve was generated, the pixel abscissa was replaced with the evaluated calibration curve's approximation for the wavelength abscissa. After the first conversion, the spectrum was then lined up with the spectrometer's abscissa. Since the evaluated calibration curve abscissa for the first conversion did not linearly line up with the spectrometer's abscissa, the abscissa of the evaluated calibration curve was resampled by linearly interpolating between the indices in the calibration. With an increased sample set, the line-up procedure can preserve the shape of the spectrum, the relative intensities, and the positions of the peaks, in terms of wavelength.

As predicted in Table 3.7, 16 interference free atomic lines of trace elements were identified in the surrogate nuclear melt glass and Trinitite samples (Figures 6-9). Small deviations were found in the spectra comparison where some intensities of certain trace elements were either slightly higher or lower than their respective counterparts in other sample types due to non-heterogeneity of trace element distribution within the samples as well as some of the previously described data collection methods. No emission lines for any trace element were found between 340-380 nm.

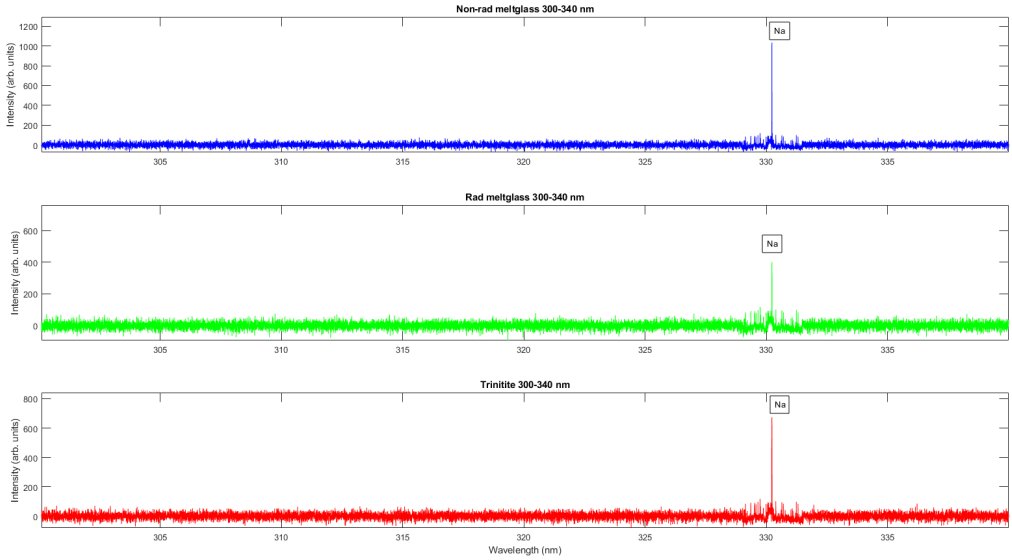


Figure 6: Comparison of fs-LIBS spectra of non-radioactive melt glass (blue), radioactive melt glass (green), & Trinitite (red) from 300-340 nm.

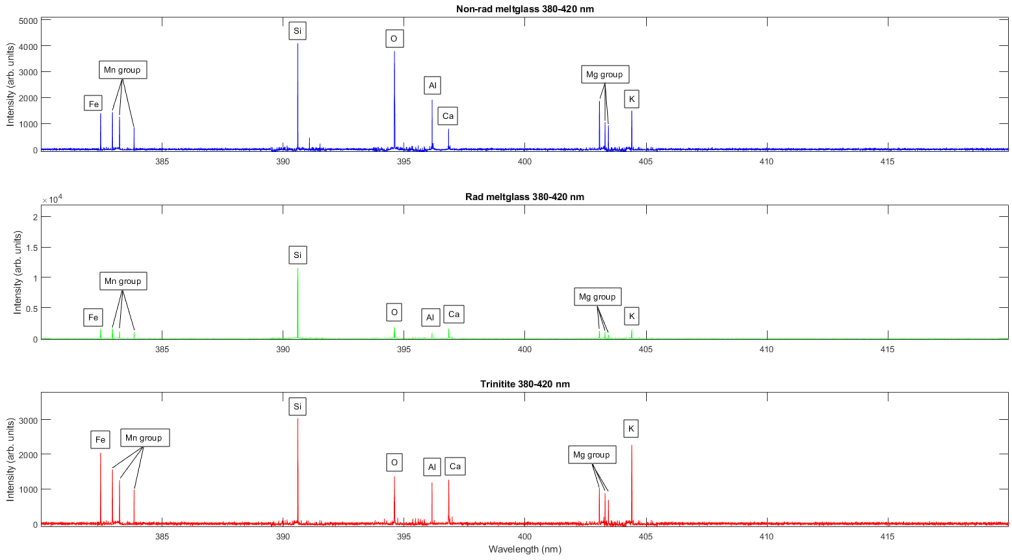


Figure 7: Comparison of fs-LIBS spectra of non-radioactive melt glass (blue), radioactive melt glass (green), & Trinitite (red) from 380-420 nm.

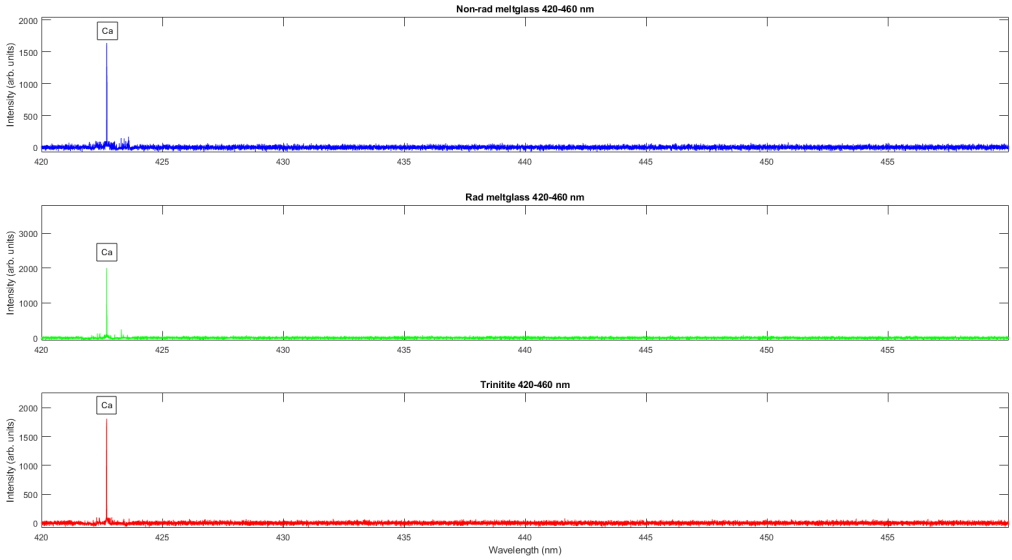


Figure 8: Comparison of fs-LIBS spectra of non-radioactive melt glass (blue), radioactive melt glass (green), & Trinitite (red) from 420-460 nm.

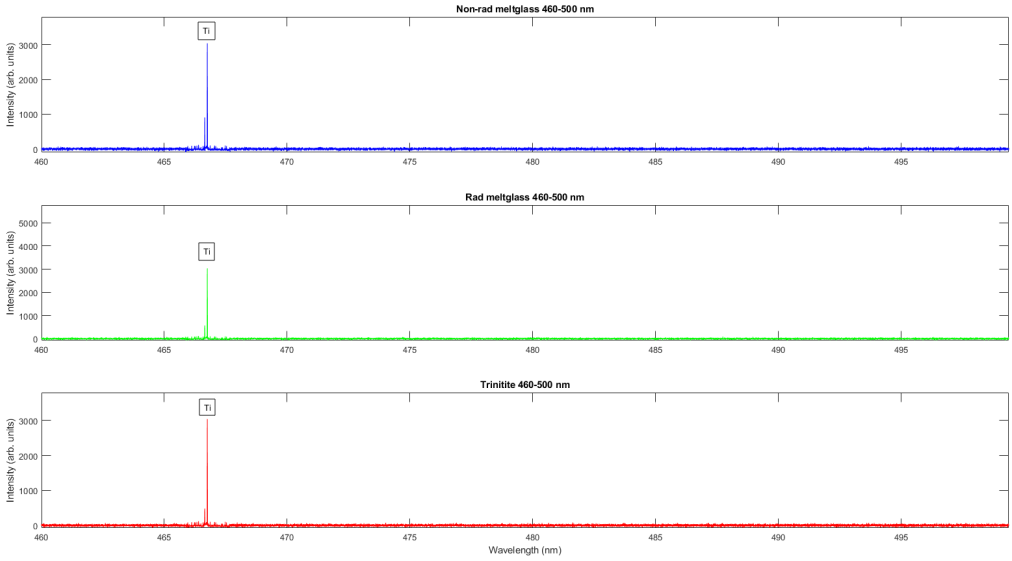


Figure 9: Comparison of fs-LIBS spectra of non-radioactive melt glass (blue), radioactive melt glass (green), & Trinitite (red) from 460-500 nm.

Since natural Uranium was used in the Tamper Device inside the Trinity atomic bomb, the little amount of $U_{235}$ would be lower following the Trinity Test Detonation due to the fission of $U_{235}$ atoms. As a result, it was deemed highly unlikely that $U_{235}$ peaks could be found in either the radioactive nuclear melt glass or Trinitite Samples. After consulting past LIBS of Uranium spectra for $U_{235}$ peaks and conducting the fs-LIBS experiments, this hypothesis was found to be accurate. Since Uranium was very trace in both the Radioactive Nuclear Melt Glass and Trinitite Samples, there were limitations in confidently acquiring Uranium-rich deposits within the various samples. Upon reviewing the collected

spectra, it was determined that further fs-LIBS on samples with well established Uranium isotopic data of varying enrichment levels would be required to confidently attribute emission peaks to specific isotopes of Uranium and conduct isotopic shift measurements. Complicated calibration of the uranium spectra needs to be undertaken, and the types of peaks that were found in radioactive melt glass and Trinitite were either so low that they could not be separated from the noise floor or they were so broad that they could not be used for calibration. Current calibration methods for Uranium spectra require at least three relatively sharp peaks present in the spectral window of the ICCD.

## SUMMARY & FUTURE WORK

Over 75 years since the Trinity atomic bomb test in 1945, the need for accurate and fast post-detonation nuclear forensics analytical techniques is needed to combat the present-day global nuclear proliferation and terrorism threats. This research has reaffirmed the great potential that fs-LIBS continues to hold within the nuclear forensics industry. Furthermore, a novel comparison of the fs-LIBS spectra of trace elements found in radioactive/non-radioactive nuclear melt glass and Trinitite has been demonstrated. 16 interference free atomic emission lines of ten trace elements were found in each of the surrogate nuclear debris and Trinitite samples.

From the work of Cook et al., it was shown that while past research on gamma spectroscopy had yielded gamma-ray emission peaks for Ba-133, Cs-137, Eu-152, Eu-154, Eu-155, Pu-239, Pu-241, Am-241, and Co-60 in Trinitite, the Cs-137 gamma emission peak was the only comparable peak between Trinitite and thermal neutron irradiated (at High Flux Isotope Reactor (HFIR) at ORNL) nuclear melt glass that could be found today due to the half-lives of these radioisotopes of interest and the lack of enriched Uranium or Plutonium in the surrogate samples [29]. Further investigation for the activation and fission products in Trinitite is warranted since no previous research has probed Trinitite with fs-LIBS, and the only elements examined with ns-LIBS are Si, Mg, Al, Ca, Ti, Na, H, N, K, and O, as mentioned earlier in this research [24].

Additional research would be to use the slope of the wavelength calibration line to calculate the Limit of Detection (LOD) for each of the trace elements found in the radioactive/non-radioactive nuclear melt glass and Trinitite samples. Past LIBS research has yielded LODs in the parts per billion (ppb) range which is highly comparable to mass spectrometry whose LODs have resulted in the range of parts per trillion (ppt) [31,32].

The current inventory of non-radioactive and radioactive surrogate nuclear melt glass at UTK needs to be replenished with additional synthesized samples with preparation techniques and elemental composition from past work such as ones developed by Molgaard et al [27]. Moreover, additional Trinitite samples should be purchased from a variety of authorized online retailers. Acquiring more of each of these three samples will allow for additional comparative LIBS analysis to further explore additional elements that could be found in surrogate nuclear melt glass or Trinitite. Furthermore, new sample preparation methods could be developed to include enriched Uranium or Plutonium to compare the distribution of activation and fission products as well as improving the accuracy of determining interference free isotopic lines of Uranium more accurately in surrogate nuclear debris and Trinitite.

## ACKNOWLEDGEMENTS

*This material is based upon work supported by the Department of Energy National Nuclear Security Administration through the Nuclear Science and Security Consortium under Award Number* DE-NA0003180.

*This conference paper was prepared as an account of work sponsored by an agency of the United States Government. Neither the United States Government nor any agency thereof, nor any of their employees, makes any warranty, express or limited, or assumes any legal liability or responsibility for the accuracy, completeness, or usefulness of any information, apparatus, product, or process disclosed, or represents that its use would not infringe privately owned rights. Reference herein to any specific commercial product, process, or service by trade name, trademark, manufacturer, or otherwise does not necessarily constitute or imply its endorsement, recommendation, or favoring by the United States Government or any agency thereof. The views and opinions of the author expressed herein do not necessarily state or reflect those of the United States Government or any agency thereof.*

## REFERENCES

[1] Radziemski L.J. (1983), 'Detection of beryllium by laser-induced breakdown spectroscopy', *Spectrochimica Acta Part B-Atomic Spectroscopy*, **38**, 349–355.
[2] Kim Y S, Han B Y, Shin H S, Kim H D, Jung E C, Jung J H and Na S H 2012 Determination of uranium concentration in an ore sample using laser-induced breakdown spectroscopy Spectrochim. Acta B 74–5 190–3.
[3] Judge E J, Barefield J E, Berg J M, Clegg S M, Havrilla G J, Montoya V M, Le L A and Lopez L N 2013 Laser-induced breakdown spectroscopy measurements of uranium and thorium powders and uranium ore Spectrochim. Acta B 83–4 28–36.
[4] Barefield J E, Judge E J, Campbell K R, Colgan J P, Kilcrease D P, Johns H M, Wiens R C, McInroy R E, Martinez R K and Clegg S M 2016 Analysis of geological materials containing uranium using laser-induced breakdown spectroscopy Spectrochim. Acta B 120 1–8.
[5] Klus J, Mikysek P, Prochazka D, Pořízka P, Prochazková P, Novotný J, Trojek T, Novotný K, Slobodník M and Kaiser J 2016 Multivariate approach to the chemical mapping of uranium in sandstone-hosted uranium ores analyzed using double pulse laser-induced breakdown spectroscopy Spectrochim. Acta B 123 143–9.
[6] Sirven J-B, Pailloux A, M'Baye Y, Coulon N, Alpettaz T and Gossé S 2009 Towards the determination of the geographical origin of yellowcake samples by laser-induced breakdown spectroscopy and chemometrics J. Anal. At. Spectrom. 24 451–9.
[7] Campbell K R, Wozniak N R, Colgan J P, Judge E J, Barefield J E, Kilcrease D P, Wilkerson M P, Czerwinski K R and Clegg S M 2017 Phase discrimination
of uranium oxides using laser-induced breakdown spectroscopy Spectrochim. Acta B 134 91–7.
[8] Sarkar A, Alamelu D and Aggarwal S K 2009 Laser-induced breakdown spectroscopy for determination of uranium in thorium-uranium mixed oxide fuel materials Talanta 78 800–4.
[9] Fichet P, Mauchien P and Moulin C 1999 Determination of impurities in uranium and plutonium dioxides by laser-induced breakdown spectroscopy Appl. Spectrosc 53 1111–7.
[10] Campbell K R, Judge E J, Barefield J E, Colgan J P, Kilcrease D P, Czerwinski K R and Clegg S M 2017 Laser-induced breakdown spectroscopy of light water reactor simulated used nuclear fuel: main oxide phase Spectrochim. Acta B 133 26–33.
[11] Singh M, Sarkar A, Banerjee J and Bhagat R K 2017 Analysis of simulated high burnup nuclear fuel by laser-induced breakdown spectroscopy Spectrochim. Acta B 132 1–7.
[12] Williams A N and Phongikaroon S 2016 Elemental detection of cerium and gadolinium in aqueous aerosol via laser-induced breakdown spectroscopy Appl. Spectrosc. 70 1700–8.
[13] Wachter J R and Cremers D A 1987 Determination of uranium in solution using laser-induced breakdown spectroscopy Appl. Spectrosc. 41 1042–8.
[14] Sarkar A, Alamelu D and Aggarwal S K 2008 Determination of thorium and uranium in solution by laser-induced breakdown spectrometry Appl. Opt. 47 G58–64.
[15] Sarkar A, Telmore V M, Alamelu D and Aggarwal S K 2009 Laser-induced breakdown spectroscopic quantification of platinum group metals in simulated high-level nuclear waste J. Anal. At. Spectrom. 24 1545.
[16] Williams A N and Phongikaroon S 2017 Laser-induced breakdown spectroscopy (LIBS) in a novel molten salt aerosol system Appl. Spectrosc. 71 744–9.
[17] Sarkar A, Mishra R K, Kaushik C P, Wattal P K, Alamelu D and Aggarwal S K 2014 Analysis of barium borosilicate glass matrix for uranium determination by using ns-IRLIBS in air and Ar atmosphere Radiochim. Acta 102 805–12.

[18] Jung E C, Lee D H, Yun J I, Kim J G, Yeon J W and Song K 2011 Quantitative determination of uranium and europium in glass matrix by laser-induced breakdown spectroscopy Spectrochim. Acta B 66 761–4.
[19] Lang A et al 2018 Analysis of contaminated nuclear plant steel by laser-induced breakdown spectroscopy J. Hazard. Mater. 345 114–22.
[20] Doucet F R, Lithgow G, Kosierb R, Bouchard P and Sabsabi M 2011 Determination of isotope ratios using laser-induced breakdown spectroscopy in ambient air at atmospheric pressure for nuclear forensics J. Anal. At. Spectrom. 26 536.
[21] Cremers D A, Beddingfield A, Smithwick R, Chinni R C, Jones C R, Beardsley B and Karch L 2012 Monitoring uranium, hydrogen, and lithium and their isotopes using a compact laser-induced breakdown spectroscopy (LIBS) probe and high-resolution spectrometer Appl. Spectrosc. 66 250–61.
[22] Shattan, M. B., Gragston, M., Zhang, Z., Auxier, J. D., McIntosh, K. G., & Parigger, C. G. (2019). Mapping of Uranium in Surrogate Nuclear Debris Using Laser-Induced Breakdown Spectroscopy (LIBS). Applied Spectroscopy, 73(6), 591–600. https://doi.org/10.1177/0003702819842871.
[23] R. Chinni, D.A. Cremers, R. Multari. ‘‘Analysis of Material Collected on Swipes Using Laser-Induced Breakdown Spectroscopy’’. Appl. Opt. 2010. 49(13): C143–C152.
[24] Appendix D: Examples of LIBS Spectra - Handbook of Laser-Induced Breakdown Spectroscopy - Wiley Online Library. https://onlinelibrary.wiley.com/doi/pdf/10.1002/9781118567371.app4
[25] F.J. Fortes, J.J. Laserna, The development of fieldable laser-induced breakdown spectrometer: No limits on the horizon, Spectrochimica Acta Part B: Atomic Spectroscopy, Volume 65, Issue 12, 2010, Pages 975-990, ISSN 0584-8547, https://doi.org/10.1016/j.sab.2010.11.009.
[26] Verhoff, B., Harilal, S. S., J. R. Freeman, P. K. Diwakar, and A. Hassanein. “Dynamics of Femto- and Nanosecond Laser Ablation Plumes Investigated Using Optical Emission Spectroscopy.” AIP Publishing. American Institute of Physics, November 1, 2012. https://aip.scitation.org/doi/10.1063/1.4764060.
[27] Molgaard, Joshua J et al. “Production of Synthetic Nuclear Melt Glass.” Journal of visualized experiments: JoVE 107 (2016): n. pag. Web.
[28] Online NIST LIBS Database https://physics.nist.gov/PhysRefData/ASD/LIBS/libs-form.html
[29] Cook, M.T., Auxier, J.D., Giminaro, A.V. *et al.* A comparison of gamma spectra from trinitite versus irradiated synthetic nuclear melt glass. *J Radioanal Nuclear Chem* **307,** 259–267 (2016). https://doi.org/10.1007/s10967-015-4266-3.
[30] Hartman, Jonathan Daniel, “The Development and Implementation of a Testing Regime for a Laser Spectroscopy Sample Chamber.” MS Thesis, University of Tennessee, 2021.
[31] He, Yage et al. “Lithium ion detection in liquid with low detection limit by laser-induced breakdown spectroscopy.” *Applied optics* vol. 58,2 (2019): 422-427. doi:10.1364/AO.58.000422
[32] Arnquist, Isaac J et al. “Mass Spectrometric Determination of Uranium and Thorium in High Radiopurity Polymers Using Ultra Low Background Electroformed Copper Crucibles for Dry Ashing.” *Analytical chemistry* vol. 89,5 (2017): 3101-3107. doi:10.1021/acs.analchem.6b04854